Available online at www.sciencedirect.com
ScienceDirect
Trans. Nonferrous Met. Soc. China 19(2009) 525−529
Transactions of Nonferrous Metals Society of China
www.tnmsc.cn

# Isothermal oxidation behavior of $Ti_3Al$-based alloy at 700−1 000 ℃ in air

QIAN Yu-hai(钱余海)[1, 2], LI Mei-shuan(李美栓)[2], LU Bin(卢 斌)[2]

1. R & D Center, Baoshan Iron & Steel Co, Ltd, Shanghai 201900, China;
2. Shenyang National Laboratory for Materials Science, Institute of Metals Research, Chinese Academy of Sciences, Shenyang 110016, China

Received 18 July 2008; accepted 28 September 2008

**Abstract:** The isothermal oxidation behavior of a $Ti_3Al$-based alloy (Ti-24Al-14Nb-3V-0.5Mo-0.3Si, molar fraction, %) at 700−1 000 ℃ in air was investigated. The oxidation kinetics of tested alloy approximately obeys the parabolic law, which shows that the oxidation process is dominated by the diffusion of ions. The oxidation diffusion activity energy is 241.32 kJ/mol. The tested alloy exhibits good oxidation resistance at 700 ℃. However, when the temperature is higher than 900 ℃, the oxidation resistance becomes poor. The XRD results reveal that the oxide product consists of a mixture of $TiO_2$ and $Al_2O_3$. Serious crack and spallation of oxide scale occur during cooling procedure after being exposed at 1 000 ℃ in air for 16 h. According to the analysis of SEM/EDS and XRD, it is concluded that the $Al_2O_3$ oxide forms at the initially transient oxidation stage and most of it keeps in the outer oxide layer during the subsequent oxidation procedure.

**Key words:** oxidation resistance; $Ti_3Al$-based intermetallic alloy; oxidation kinetics

## 1 Introduction

With outstanding properties, intermetallics such as $Ti_3Al$ and TiAl may act as potential structural materials serving under high temperature environments[1−2] and are paid much attention extensively. However, there are some disadvantages for intermetallics, such as brittleness and poor working performance at room temperature. What's more, oxidation resistance of intermetallics with Ti-Al system was poor at 650 ℃ and above[3]. Much research showed that addition of alloying elements and application of protective coating might improve oxidation resistance of Ti-Al system intermetallics effectively[1,4−8]. For the oxidation behavior of $Ti_3Al$-based alloys, many research results showed that a mixture oxide consisting of main $TiO_2$ rather than protective $Al_2O_3$ was produced and their oxidation kinetics was very complicated[9−12].

For structural materials at high temperature, their high temperature oxidation resistance is a very important aspect during their service life. In this work, the oxidation behaviors of a kind of $Ti_3Al$-based alloy was investigated to evaluate its oxidation resistance in the temperature range of 700−1 000 ℃ in static air. Meanwhile, the formation mechanism of oxide scale and the effect of addition of Nb on the oxidation behavior were discussed.

## 2 Experimental

The $Ti_3Al$-based alloy, Ti-24Al-14Nb-3V-0.5Mo-0.3Si (molar fraction, %), for test was provided by Institute of Metals Research, Chinese Academy of Sciences. The processing methods were as follows. Alloy ingots were obtained after melting two times in vacuum consumable electrode furnace. The ingots were wrought at $\beta$-single phase area firstly and then at ($\alpha_2$+$\beta$) double-phase areas. Round rods with diameter of 21 mm were produced. The heat treatment schemes after forging procedure were 1 000 ℃, 1 h, AC and 850 ℃, 2 h, AC, respectively.

Square specimens with dimensions of 10 mm×2 mm were cut by electrical-discharge method. The surfaces of specimens were ground down to 800# SiC paper. The samples were cleaned in acetone and alcohol

**Foundation item:** Project(50771099) supported by the National Natural Science Foundation of China
**Corresponding author:** QIAN Yu-hai; Tel: +86-21-26649568; Fax: +86-21-26649556; E-mail: yhqian@baosteel.com
DOI: 10.1016/S1003-6326(08)60306-4

in an ultra-sonic bath before testing.

The oxidation test was performed at 700−1 000 ℃ in static air. The continuous measurements of isothermal mass gain were conducted at 700, 800, 900 and 1 000 ℃ in air for 16 h. The sample was suspended in a thermobalance with a Pt wire. The mass gain was recorded automatically. The phase composition of oxide layer was determined by X-ray diffractometer(XRD). The morphology of surface oxide was investigated using scanning electron microscope(SEM) equipped with energy dispersive spectroscope(EDS).

## 3 Results

### 3.1 Kinetics of oxidation

Fig.1(a) shows the kinetic curves of samples during the oxidation in air at 700−1 000 ℃ for 16 h. For the case of oxidation at 700 ℃, the mass gain was very slow and the total mass gain per unit area was 0.183 mg/cm$^2$, so the tested alloy exhibited good oxidation resistance at 700 ℃. However, when the temperature was higher than 900 ℃, the mass gain was very large and its oxidation resistance was poor. Fig.1(b) reveals the relationship between the square of mass gain per unit area and oxidation time. According to Fig.1(b), the oxidation kinetics of tested alloy at all temperatures approximately obeyed parabolic law.

### 3.2 Phase composition and microstructure of oxide

Fig.2 shows the surface morphologies of specimens

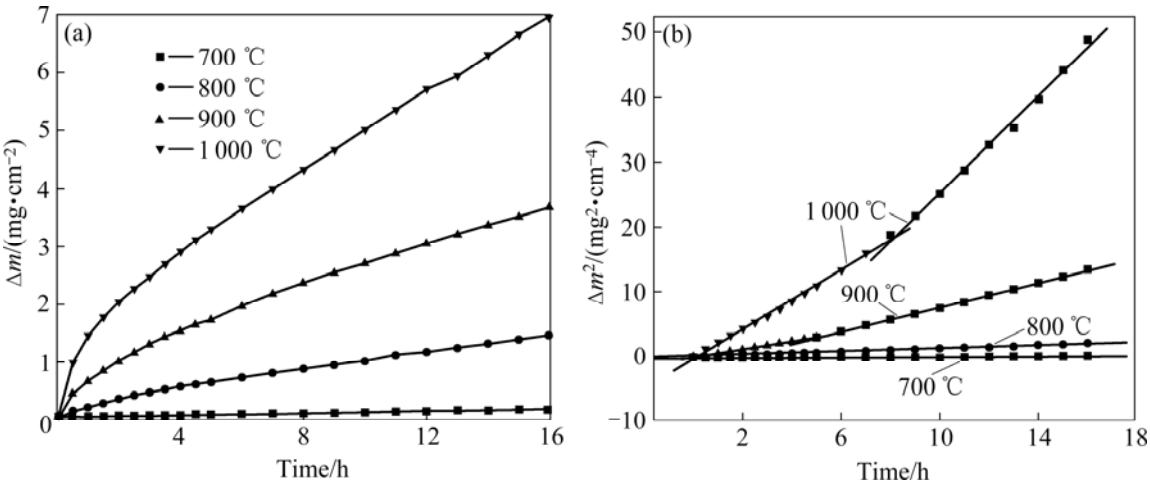


**Fig.1** Oxidation kinetic curves of alloy during oxidation in air at 700−1 000 ℃ for 16 h: (a) Mass gain versus time; (b) Square of mass gain versus time

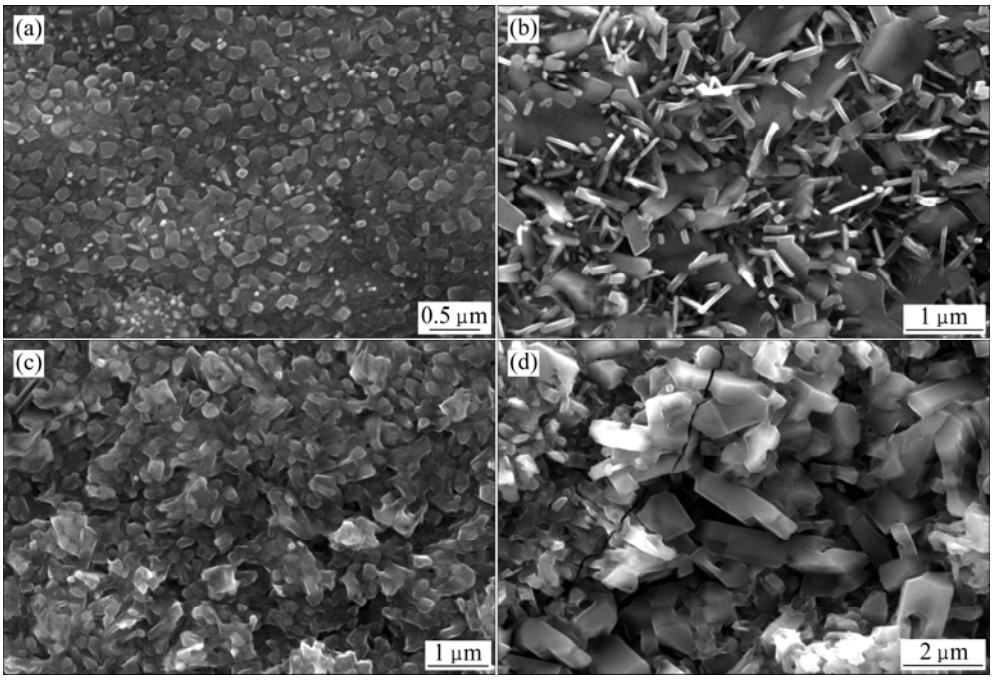


**Fig.2** Surface morphologies of alloy after oxidation for 16 h at 700 ℃ (a), 800 ℃ (b), 900 ℃ (c), and 1 000 ℃ (d)

after oxidation for 16 h in air at 700−1 000 ℃. In the cases lower than 900 ℃, the oxide scale was compact and no crack and spallation were observed. Serious crack and spallation of oxide scale occurred at 1 000 ℃. Fig.2(d) shows the local magnification of non-spallation areas and many micro-cracks were found. The surface morphologies changed from the initial granular to transient flake-like and then to columnar in the end during oxidation from 700 ℃ to 1 000 ℃.

Fig.3 shows the cross-section morphologies of oxide layer after oxidation at 700−1 000 ℃ in air for 16 h. For the case of 1 000 ℃, serious spallation led to a great difference between the mass gain of oxide in oxidation kinetics and the corresponding thickness of the oxide layer.

Table 1 shows the EDS analysis results corresponding to different spots marked in Fig.3(c) and Fig.3(d). Fig.4 shows the XRD pattern of sample after oxidation for 16 h at 900 ℃ in air. XRD analysis revealed that the main crystalline phase was mixture oxide consisting of $Al_2O_3$ and $TiO_2$.

## 4 Discussion

When characterizing the oxidation rate of alloy, it is usually suggested that oxidation behavior obeys simple oxidation law. The relationship between the mass gain and oxidation time can be expressed as

$$(\Delta m)^n=kt \tag{1}$$

where $\Delta m$ is the mass gain per unit area; $k$ is the oxidation rate constant; $n$ is the exponent of oxidation rate; and $t$ is the oxidation time.

As shown in Fig.1(b), the oxidation kinetics of the samples approximately obeys the parabolic law, so the oxidation process is dominant by diffusion process of ions. The oxidation rate can be described as $(\Delta m)^2=k_p t$, where the oxidation rate constant $k_p$ is the function of oxidation temperature and $k_p$ agrees with the Arrhenius relationship:

$$k_p=k_0\exp[(-Q/RT)] \tag{2}$$

where $k_0$ is a constant, $Q$ is the activity energy and $T$ is the absolute temperature.

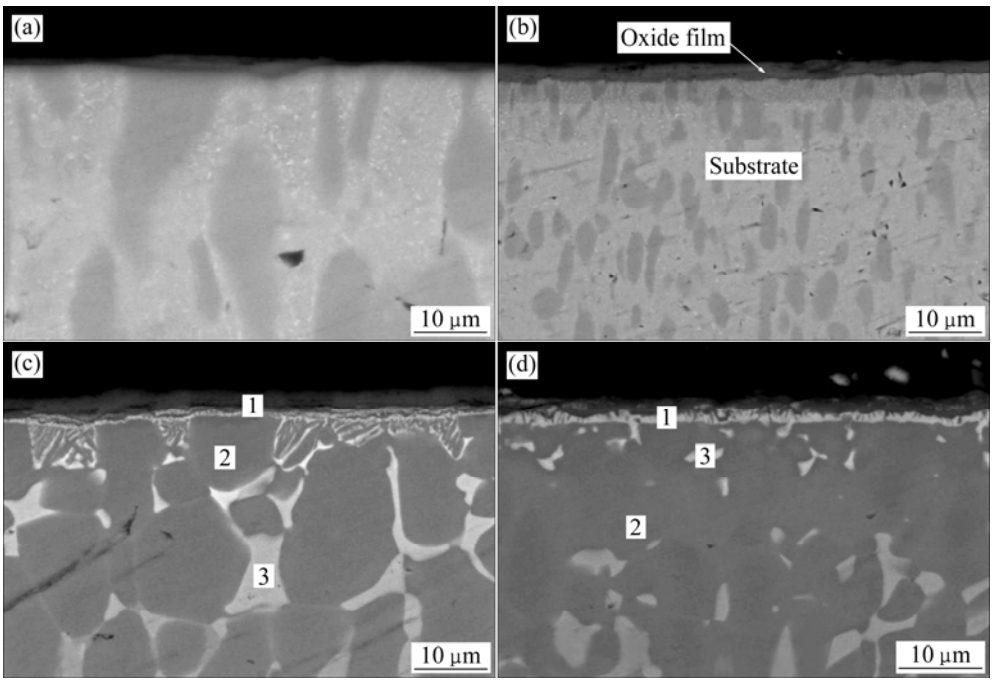


**Fig.3** Cross-section morphologies of oxide layer for alloy after oxidation for 16 h at different temperatures: (a) 700 ℃; (b) 800 ℃; (c) 900 ℃; (d) 1 000 ℃

**Table 1** EDS results for different spots marked in Fig.3(c) and Fig.3(d) (mass fraction, %)

| Element | Fig.3(c) | | | Fig.3(d) | | |
|---|---|---|---|---|---|---|
| | Spot 1 | Spot 2 | Spot 3 | Spot 1 | Spot 2 | Spot 3 |
| Al | 17.39 | 17.33 | 12.63 | 18.55 | 16.35 | 13.36 |
| Nb | 38.45 | 22.12 | 46.75 | 46.04 | 25.64 | 39.36 |
| Ti | 44.16 | 60.55 | 40.62 | 35.42 | 58.00 | 47.28 |

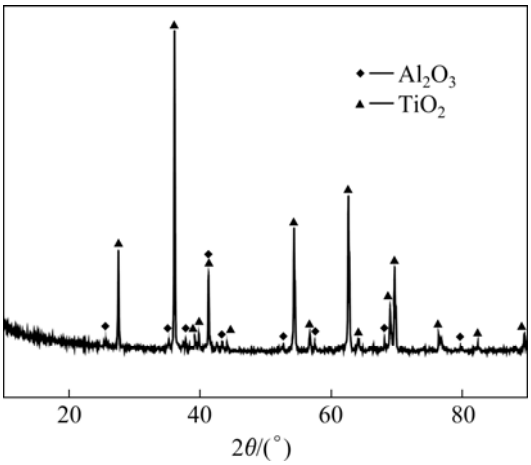


**Fig.4** XRD pattern of sample oxidized at 900 ℃ in air for 16 h

Values of the oxidation rate constant $k_p$ under different oxidation temperatures are listed in Table 2.

**Table 2** Oxidation rate constant $k_p$ of alloy at different temperatures

| Temperature/℃ | $k_p$/(mg$^2$·cm$^{-4}$·s$^{-1}$) |
|---|---|
| 700 | $5.44\times10^{-7}$ |
| 800 | $3.63\times10^{-5}$ |
| 900 | $1.72\times10^{-4}$ (0−5 h)<br>$2.63\times10^{-4}$ (5−16 h) |
| 1 000 | $6.41\times10^{-4}$ (0−8 h)<br>$1.04\times10^{-3}$ (8−16 h) |

The diffusion activation energy during oxidation procedure may be calculated according to slope of lines in lg$k_p$−1/$T$ plots shown in Fig.5. The oxidation diffusion activity energy is 241.32 kJ/mol and it is similar to the value of 259 kJ/mol for $Ti_3Al$.

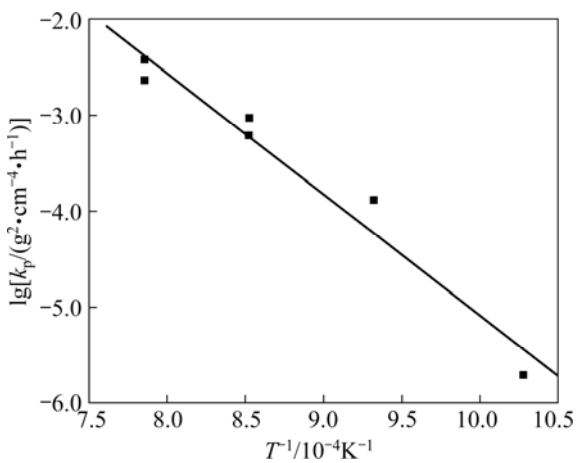


**Fig.5** Arrhenius plot of $k_p$ with oxidation temperature

Due to the significantly negative deviation between the activity of Al element and its real molar content, for intermetallics of Ti-Al system, bi-layered mixture oxide film consisting of $TiO_2$ and $Al_2O_3$ rather than a single protective $Al_2O_3$ oxide is usually produced[13], so their oxidation resistances are poor.

$TiO_2$ is non-stoichiometric and defects exist among lattice structure. The oxidation transporting process will be affected by the defects. As the dominant point defects in $TiO_2$ are vacancies of oxygen atom and interval titanium ions ($Ti_i^{\bullet\bullet\bullet}$ or $Ti_i^{\bullet\bullet\bullet\bullet}$), the non-stoichiometry can be described as $Ti_{1+x}O_{2-y}$, and it is well accepted that the inward $O^{2-}$ diffusion is dominant.

Table 3 lists the EDS results of oxide formed at 1 000 ℃ in air for 16 h. For the non-spallation area, the oxide was enriched with Ti and Al elements. On the contrary, for the spallation area, the Nb element was high and no Al element was detected. The growth of $TiO_2$ was dominant by inward diffusion of oxygen, so the growth of new oxide mainly occurred at alloy/oxide interface, rather than oxide/air interface. The fact that Al element appeared only in outer layer of oxide film showed that $Al_2O_3$ formed at initial oxidation stage, which was in agreement with the result revealed by XPS for the initial stages of oxidation of $\alpha_2$-$Ti_3Al$ and $\gamma$-TiAl intermetallic alloys[9]. And it could be deduced that a mixture of $Al_2O_3$ and $TiO_2$ formed at initial stage, but $Al_2O_3$ was non-continuous. Then, $TiO_2$ continued to form by the inward diffusion of oxygen ions through the non-continuous $Al_2O_3$ oxide. During this process, less part of $Al_2O_3$ oxide would be incorporated with $TiO_2$ and the most of $Al_2O_3$ would be kept in the outer layer. So, the quantity of Al element in the outer oxide layer was high.

**Table 3** EDS results of oxide formed at 1 000 ℃ in air for 16 h (mass fraction, %)

| Element | Spallation area | Non-spallation area |
|---|---|---|
| O | 17.68 | 23.06 |
| Nb | 26.38 | 5.49 |
| Ti | 55.94 | 45.73 |
| Al | − | 25.72 |

During the process of isothermal oxidation, growth stress in the oxide is dominant. For the $Al_2O_3$ film formed on MCrAlY system, the growth stress can be negligible[14]. However, growth stress in $TiO_2$ is significant[15]. Severe cracking and spallation occurred due to the combination of significant growth stress and thermal stress during the cooling process from 1 000 ℃ to room temperature.

Addition of alloying element such as Nb will increase the activity of Al element in $Ti_3Al$ alloy and the critical Al concentration to produce $Al_2O_3$ is expected to decrease. So, Nb accelerates the selective oxidation of $Ti_3Al$. However, compared with the Arrhenius

relationship curves for the $Al_2O_3$-forming kinetics[16], the oxidation kinetics agreed with the $TiO_2$-forming Arrhenius relation rather than the $Al_2O_3$-forming one. So, the oxidation process was dominated by the $TiO_2$-forming kinetics.

According to results of XRD and EDX, the oxide product contained Nb element. The possible existing state of Nb element in the oxide layer is either solid solution or other ways. As far as n-type semi-conductor was concerned, the growth of $TiO_2$ was dominant by the outward transportation of oxygen vacancy. Because the valence of $Nb^{5+}$ is higher than $Ti^{4+}$, according to the theory of electrical neutrality, the doping effect of $Nb^{5+}$ will decrease the concentration of oxygen vacancy in oxide, so the transporting rate of oxygen vacancy becomes lower. The depressed oxygen transportation will lead to an enhancement of oxidation resistance.

The maximum solubility of Nb in $TiO_2$ is approximately 5% (molar fraction) at 1 400 ℃. It is concluded that solubility of Nb in $TiO_2$ at 700−1 000 ℃ is much lower than that at 1 400 ℃. During oxidation process, Nb will dissolve in $TiO_2$ up to its maximum solubility. As mentioned above, doping effects of Nb leads to a decrease of concentration of oxygen vacancy, so the addition of Nb element will improve the oxidation resistance.

## 5 Conclusions

1) Ti-24Al-14Nb-3V-0.5Mo-0.3Si (molar fraction, %) exhibits good oxidation resistance at 700 ℃. However, when the temperature is higher than 900 ℃, its oxidation resistance becomes poor. The oxidation kinetics of alloy approximately obeys parabolic law. The oxidation diffusion activity energy of sample is about 241.32 kJ/mol. The oxidation process is dominated by the growth of $TiO_2$.

2) The oxide mixture consisting of $TiO_2$ and $Al_2O_3$ forms during oxidation process. The combination of significant growth stress and thermal stress leads to crack and spallation of oxide scale during cooling process.

3) An oxide scale mainly consisting of $TiO_2$ with non-continuous $Al_2O_3$ oxide forms during transient oxidation stage. During the subsequent oxidation procedure, $TiO_2$ grows by inward oxygen diffusion and $Al_2O_3$ mainly keeps in the outer oxide layer.

## References


[1] CHEN Yun-feng, XIONG Hua-ping, MAO Wei. Improvement on high-temperature oxidation resistance of a $Ti_3Al$-based alloy by liquid-phase silicon-aluminizing [J]. Corrosion Science and Protection Technology (China), 2005, 17( 1): 39−42. (in Chinese)

[2] CHU M S, WU S K. Improvement in the oxidation resistance of $\alpha_2$-$Ti_3A1$ by sputtering Al film and subsequent interdiffusion treatment [J]. Surface Coating Technology, 2004, 179(2/3): 257−264.

[3] KOO C H, YU T H. Pack cementation coatings on $Ti_3A1$-Nb alloys to modify the high-temperature oxidation properties [J]. Surface and Coatings Technology, 2000, 126(2/3): 171−180.

[4] XIONG Yu-ming, GUAN Chun-hong, ZHU Sheng-long, WANG Fu-hui. Effect of enamel coating on oxidation and hot corrosion behaviors of Ti-24Al-14Nb-3V alloy [J]. Journal of Materials Engineering and Performance, 2006, 15(5): 564−569. (in Chinese)

[5] LI Z, GAO W, YOSHIHARA M, HE Y. Improving oxidation resistance of $Ti_3Al$ and TiAl intermetallic compounds with electro-spark deposit coatings [J]. Materials Science and Engineering A, 2003, 347(1/2): 243−252.

[6] XIONG H P, XIE Y H, MAO W, CHEN Y F, LI X H. Liquid-phase siliconizing and aluminizing at the surface of a $Ti_3Al$-based alloy and improvement in oxidation resistance [J]. Journal of Materials Research, 2004, 19(4): 1050−1057.

[7] JAZAYERI G A, BUCKLEY R A, DAVIES H A. Microstructure and oxidation resistance of rapidly solidified $Ti_3Al$-Si alloys [J]. Materials Science and Technology, 2002, 18(12): 1485−1493.

[8] LI Z W, GAO W, YING D Y, ZHANG D L. Improved oxidation resistance of Ti with a thermal sprayed $Ti_3Al(O)$-$Al_2O_3$ composite coating [J]. Scripta Materialia, 2003, 48(12): 1649−1653

[9] MAURICE V, DESPERT G, ZANNA S, JOSSO P, BACOS M P, MARCUS P. XPS study of the initial stages of oxidation of $\alpha_2$-$Ti_3Al$ and $\gamma$-TiAl intermetallic alloys [J]. Acta Materialia, 2007, 55(10): 3315−3325.

[10] QIAN Yu-hai, LI Mei-shuan, ZHANG Ya-ming. Cyclic oxidation behaviors of $Ti_3Al$-based alloys at 700−850 ℃ in air [J]. The Chinese Journal of Nonferrous Metals, 2004, 14(9): 1609−1614. (in Chinese)

[11] QIAN Yu-hai, LI Mei-shuan, ZHANG Ya-ming. Effect of external stress on the selective oxidation of $Ti_3Al$ base alloy at 500−700 ℃ [J]. Acta Metallurgica Sinica, 2003, 39(9): 989−994. (in Chinese)

[12] REDDY R G. In-situ multi-layer formation in the oxidation of $Ti_3Al$-Nb [J]. Journal of the Minerals Metals and Materials Society, 2002, 54(2): 65−67.

[13] RAHMEL A, SPENCER P J. Thermodynamic aspects of TiAl and $TiSi_2$ oxidation: The Al-Ti-O and Si-Ti-O phase diagram [J]. Oxid Met, 1991, 35: 53−68.

[14] CHOQUET P, INDRIGO C, MEVREL R. Microstructure of oxide scales formed on cyclically oxidized M-Cr-Al-Y coating [J]. Mater Sci Eng A, 1987, 88: 97−101.

[15] BERTRAND G, JARRAYA K, CHAIX J M. Morphology of oxide scales formed on titanium [J]. Oxid Met, 1983, 21: 1−19.

[16] GIGGINS C S, PETTIT F S. Oxidation of Ni-Cr-Al alloys between 1 000 and 1 200 ℃ [J]. J Electrochem Soc, 1971, 118: 1782−1790.


**(Edited by YANG Bing)**